

GENETICS

Indigenous people from Amazon show genetic signatures of pathogen-driven selection

Cainã M. Couto-Silva^{1†}, Kelly Nunes^{1†}, Gabriela Venturini^{2,3}, Marcos Araújo Castro e Silva^{1,4}, Lygia V. Pereira¹, David Comas⁴, Alexandre Pereira^{2,3}, Tábita Hünemeier^{1,5*}

Ecological conditions in the Amazon rainforests are historically favorable for the transmission of numerous tropical diseases, especially vector-borne diseases. The high diversity of pathogens likely contributes to the strong selective pressures for human survival and reproduction in this region. However, the genetic basis of human adaptation to this complex ecosystem remains unclear. This study investigates the possible footprints of genetic adaptation to the Amazon rainforest environment by analyzing the genomic data of 19 native populations. The results based on genomic and functional analysis showed an intense signal of natural selection in a set of genes related to *Trypanosoma cruzi* infection, which is the pathogen responsible for Chagas disease, a neglected tropical parasitic disease native to the Americas that is currently spreading worldwide.

Copyright © 2023 The Authors, some rights reserved; exclusive licensee American Association for the Advancement of Science. No claim to original U.S. Government Works. Distributed under a Creative Commons Attribution NonCommercial License 4.0 (CC BY-NC).

INTRODUCTION

America presents a wide range of ecoregions that were quickly explored and occupied by the first humans to reach the continent (1). This remarkable human migration likely required different genetic and cultural adaptation patterns to ensure successful subsistence (2–5). The Amazon rainforest is one of the main ecoregions of the American continent, which is well known for its tropical climate and extraordinary biological diversity. Despite being a nutrient-rich environment, it is also hostile, presenting different obstacles to long-term human survival. Several challenges, including the instability of food resources (6, 7), low light penetration (8), and high diversity of pathogens (9), probably contribute to strong selective pressures for human survival and reproduction in this ecoregion.

The Amazon region, which encompasses the single largest tropical rainforest and nine South American countries, is virtually unrivaled in scale, complexity, and opportunity. It is currently populated by 1 million indigenous people, divided into approximately 300 different ethnic groups (10). Ecological conditions in the region have historically been favorable for transmitting numerous tropical diseases, especially vector-borne diseases (11–13). Although there are numerous studies on postcontact epidemics (14) in the Americas, historical data on precontact diseases (i.e., diseases native to the Americas) are inadequate. However, it has been reported that tuberculosis (*Mycobacterium tuberculosis*) (15, 16) and Chagas disease (i.e., American trypanosomiasis) (17) were present long before the Europeans arrived. Chagas disease is a vector-borne disease caused by the protozoan *Trypanosoma cruzi*, and it is usually transmitted through different triatomine bugs in endemic areas. The oldest record of *T. cruzi* in South American human archaeological remains dates back to 9000 years in mummies from

northern Chile and southern Peru (18). Human remains infected with *T. cruzi* were also found in Brazil about 7000 years before the present (yr B.P.) (19). There are, however, not many studies on the adaptations to the rainforest including Amazonian populations. Most of these are limited to a few individuals from the western Amazonia (20, 21). To date, knowledge regarding genetic adaptations in humans within this complex ecosystem is largely unknown. Motivated by this lack of knowledge, we searched for possible footprints of genetic adaptation to the Amazon rainforest environment by analyzing the genomic data of 118 nonadmixed individuals belonging to 19 native populations (table S1). We were specifically interested in identifying signals for positive natural selection related to tropical diseases.

To search for signals of positive selection, we applied two distinct approaches: (i) Population Branch Statistics (PBS), which identify alleles that have experienced strong changes in frequency in one population relative to two reference populations (19), and (ii) Cross-Population Extended Homozygosity Haplotype (XP-EHH) statistics, which contrast the extended haplotype homozygosity within and between populations (22). We then explored these results through gene pathway enrichment analyses [the Mapping and Annotation of Genome-Wide Association Studies (FUMA GWAS) (23), Gene Ontology (GO) (24), Kyoto Encyclopedia of Genes and Genomes (KEGG) (25), and Reactome (26) and the Gene Set Analysis Toolkit (GESTALT) (27)]. To formally test whether natural selection underlies the cases of extreme differentiation, rejecting genetic drift as a cause, PBS values were compared against those obtained with neutral coalescent simulations generated according to a plausible demographic scenario for the peopling of South America. Last, we performed a functional follow-up analysis to characterize the role of the putative selected gene.

RESULTS AND DISCUSSION

Genetic adaptation to the Amazon rainforest

The upper distribution of the combined positive selection indices (PBS + XP-EHH) is highly correlated to cardiovascular and metabolic traits (*MTRR*, *DNAJA4*, *KCMA1*, and *MTPN*), immune-related traits (*KCMA1* and *GCA*), and pathogen infection (table

¹Departamento de Genética e Biologia Evolutiva, Instituto de Biociências, Universidade de São Paulo, São Paulo, SP, 05508090, Brazil. ²Department of Genetics, Harvard Medical School, Boston, MA 02115, USA. ³Laboratório de Genética e Cardiologia Molecular, Instituto do Coração, Hospital das Clínicas da Faculdade de Medicina da Universidade de São Paulo, São Paulo, SP, Brazil. ⁴Institut de Biologia Evolutiva, Departament de Medicina i Ciències de la Vida, Universitat Pompeu Fabra, Barcelona 08003, Spain. ⁵Institut de Biologia Evolutiva (CSIC/Universitat Pompeu Fabra), Barcelona 08003, Spain.

†These authors contributed equally to this work.

*Corresponding author. Email: hunemeier@gmail.com

S2). Among the three genes that were highlighted in our analysis, *PPP3CA* and *DYNC11I* were suggestively associated with *T. cruzi* seropositivity and immune response (Fig. 1 and table S2) (28), while *NOS1AP* was related to the mosquito bite reaction (Fig. 1) (29). The strongest selection signature found in Amazonian populations was around the *PPP3CA* gene region (Fig. 1 and figs. S1 and S4). Neutral coalescent simulations indicate that these deviations in allele frequency (rs2659540 G>A) are statistically significant ($P < 0.0075$; fig. S3), which is consistent with the action of ositive selection as opposed to a genetic drift effect in the Amazonian populations. We estimated a selection starting time of 7500 yr B.P. [confidence interval (CI) = 1560 to 12,035] and a selection coefficient of 0.05 (CI = 0.015 to 0.20) (fig. S6). This result suggests that selection started acting on this gene after the split between Amazonian, Coastal Pacific, and Andes populations (30). A previous study on ancient tissues of 283 individuals, dating from 9000 to 450 yr B.P., from South America's coastal area of southern Peru and northern Chile showed a slight increase in the infection rate over time (18). These findings support our inference of a selection signal, which is likely exclusive to Amazonian rainforest populations.

The GO enrichment analysis based on both the XP-EHH (95th percentile) and PBS (95th percentile) analysis showed statistically significant enrichment of genes involved in the response to protozoan and eosinophil chemotaxis, which have a known role in parasitic infections (Table 1 and table S3). When FUMA GWAS and Enrichr were applied, associations with other traits were detected, including novelty-seeking behavior, metabolic traits, and systolic/diastolic pressure (tables S4 and S5). Several studies, including Brazilian indigenous populations, have shown high rates of obesity and cardiopathies (31, 32). For instance, in the Xavante population, 66% of individuals suffer from obesity, diabetes, or coronary heart disease (33). Bergey *et al.* (34) showed a strong signal of convergent selection in heart-related networks in studying Asian and African hunter-gatherers as compensatory adaptations to their short stature, which may possibly also be the case in Native Americans. Furthermore, we also identify associations that could raise a hypothesis for increased novelty-seeking behavior, currently recognized through caffeine and nicotine consumption (tables S4 and S5) (35, 36). Novelty-seeking behaviors may have been important in

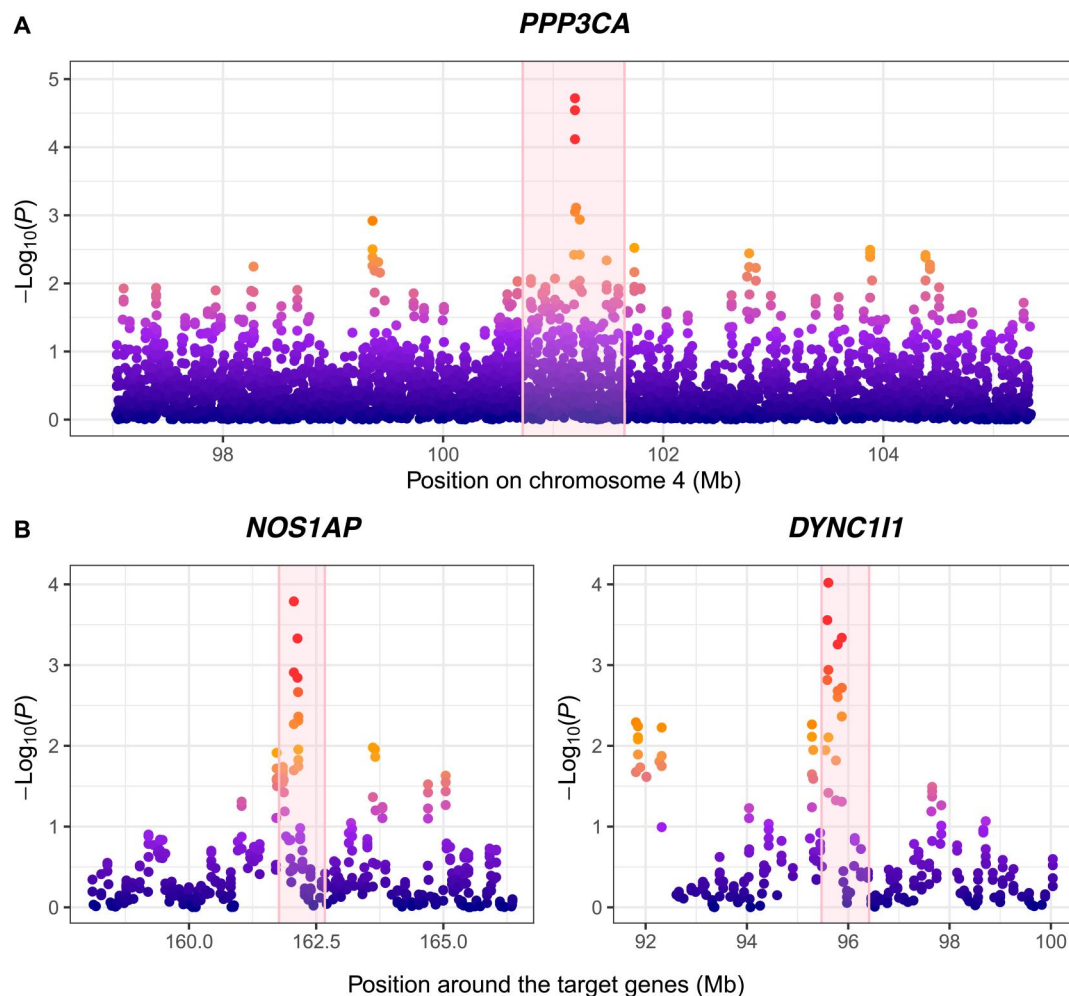


Fig. 1. PBS-windowed scores for target genes. Log_{10} of PBS P values around the (A) *PPP3CA* and (B) *NOS1AP* and *DYNC11I* genes, chromosomes 1 and 4, respectively. Graphs show up to 4 Mb away from the initial and final gene position. Pink shadow areas correspond to 300 kb of the gene limit description. All these genes have the highest PBS values for their respective chromosomes.

Table 1. Gene Ontology enrichment analysis. The extreme 95th percentile of XP-EHH and PBS distribution showed a statistically significant [false discovery rate (FDR) < 0.05, FWER < 0.1, and refine *P* value] enrichment of genes, owing to protozoan response and T cell selection.

Method	Association	<i>P</i> value FDR	FWER	Refine <i>P</i> value*
XP-EHH	Defense response to protozoan	0.01	0.08	3.25×10^{-5}
PBS	Eosinophil chemotaxis	0.008	0.03	1.61×10^{-4}
	Eosinophil migration	0.008	0.04	8.11×10^{-4}

*Remove genes FWER < 0.1 and repeat the enrichment test to check whether a significant association would still be significant.

the past to the hunter-gatherer lifestyle, helping to explore new territories and search for resources (35, 37, 38).

Functional characterization of the putative selected gene
PPP3CA encodes the protein phosphatase 3 catalytic subunit α and is involved in the G- $\beta\gamma$ signaling pathway. The G- $\beta\gamma$ complex is an essential element in the G protein-coupled receptor signaling cascade, which plays an important role in the activation of immune cells. *PPP3CA* is also involved in calcineurin signaling, a key channel in the innate immune response and *T. cruzi* internalization (39–41). The rs2659540 polymorphism is experimentally described as a regulatory variant in the Ensembl database, being active in immune cells and heart tissue (<http://ensembl.org/> on 10 May 2022).

Focusing on the association with the immunological response to protozoa, we performed a functional study of the *PPP3CA* gene in human induced pluripotent stem cell (hiPSC)-derived cardiomyocytes infected with *T. cruzi*. Using short hairpin RNAs (shRNAs) against *PPP3CA*, we found that in cells exhibiting reduced gene expression (65% reduced compared to control shRNA), *T. cruzi* significantly decreased the infectivity capacity by approximately 25% compared to control shRNA ($P < 0.0004$; Fig. 2), indicating that *PPP3CA* plays an active role in parasite intracellular infection and the disease outcome. Further, in silico analysis showed that rs2659540-derived allele (A) led to a significant reduction in the expression of *FLJ20021*, a long noncoding RNA (lncRNA) in the 3' untranslated region (3'UTR) region of the *PPP3CA* promoter, on atrial heart appendage (<https://gtexportal.org/home/snp/rs2659540> on 7 December 2022). The atrial region of the heart is primarily affected by Chagas disease (42, 43). In this sense, this gene expression reduction in the atrium could lead to a milder disease phenotype by decreasing *T. cruzi* infection. One hypothesis is that the lncRNA variant regulates differentially expressed mRNA by directly targeting *PPP3CA* 3'UTR region. However, more functional studies directly targeting the polymorphism found under natural selection are necessary to corroborate this hypothesis. Another possibility would be that this polymorphism is in linkage disequilibrium with functional variants of *PPP3CA* only in Native Americans, leading to differential expression of this gene in individuals carrying the haplotype containing the derived allele. The rs2659540 polymorphism is in strong linkage disequilibrium with

several other variants of the *PPP3CA* gene in Peruvian populations with high Native American ancestry. In African populations, this pattern of linkage disequilibrium is not found, although these populations also showed a high frequency of the derived allele (<http://ensembl.org> on 7 December 2022).

Putatively selected allele frequency in different human populations
The putatively selected allele (A) of the rs2659540 polymorphism also segregates in other geographic regions (ranging from 10% in Europe and 59% in Africa). Studies have reiterated the importance of natural selection in standing variation in local adaptation outside Africa (44). In particular, alleles with intermediate frequency and under balancing selection in Africa have the greatest potential for rapid adaptive response to environmental changes and new selective pressures in the non-African population (45). The sub-Saharan African and Amazon tropical forests have ecological similarities, including trypanosomes (*T. brucei* in Africa and *T. cruzi* in the Amazon). Therefore, a plausible hypothesis is that *PPP3CA* is associated with a response to trypanosomiasis infection in Africa and America. Once the allele is already segregating in the ancestral population, natural selection becomes effective, even with a selective coefficient of 0.05. However, it is essential to note that extended haplotype homozygosity tests do not detect a positive selection signal in the African populations in this locus (<https://pgb.ibe.upf.edu> on 7 December 2022). The lower frequency of the derived allele in Europe, South Asia, and East Asia (~10, ~15, and ~25%, respectively) may result from different evolutionary processes such as genetic drift. In addition, ecological differences between regions may trigger less selective pressure by these pathogens or even by other selective factors (e.g., negative selection—because the *PPP3CA* gene has been associated with other characteristics of clinical interest). Studies should focus on these geographic regions to better elucidate this question, preferably using whole genome sequences to avoid single-nucleotide polymorphism (SNP)-array genotyping bias.

***T. cruzi* incidence and the geographic distribution of the selected allele**
Chagas disease affects approximately 6 million people in Latin America alone and is still a leading cause of death in the region. It is also an emerging infectious disease in the United States and Europe (46), where approximately 450,000 individuals are estimated to have Chagas disease. One of the most important and unanswered questions about this disease is why only 30% of infected individuals develop chronic forms of end-stage cardiomyopathy. There is also no information about who among the infected individuals will develop heart disease later in their lives, or about the impact of genetic variants and ancestry on the disease outcome. Although the disease was already present in Amazonians in the pre-contact period, studies involving the current population have not yet reported the pathogen at a high frequency, despite the wide distribution of vectors among wild mammals and triatomines in this region (47). Serotype analysis in different Amazonian populations, such as Alto Xingu and Asuriní from Pará, Karitiana and Suruí from Rondônia, and Xavante from Mato Grosso, indicates a very low prevalence or absence of the disease. Contrarily, in Andean populations, Chagas disease is considered endemic and its frequency is high in all studied regions (48). This leads to the conclusion that

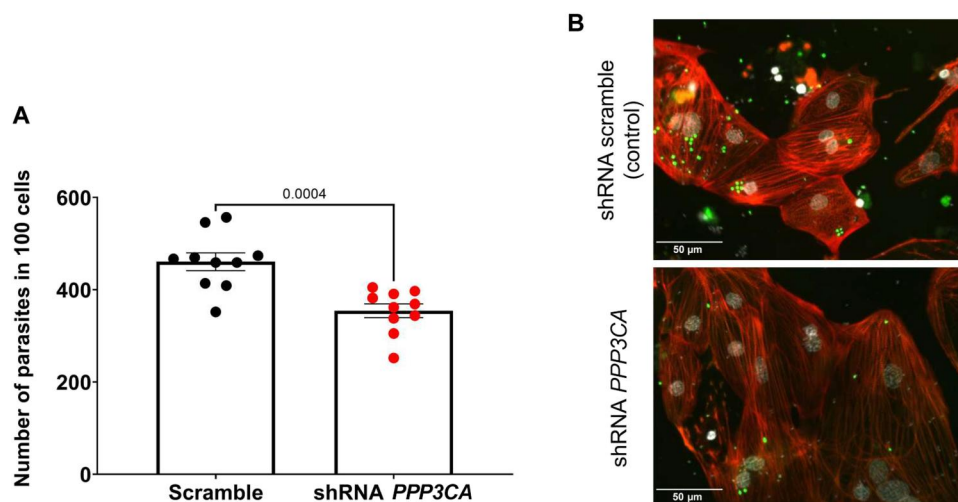


Fig. 2. Reduction in *PPP3CA* levels significantly inhibited iPS-CM *T. cruzi* infection. (A) Number of intracellular parasites per 100 cells after 24 hours of infection showing a reduction of ~25% in parasite numbers in cells with lower expression of *PPP3CA* (red). Dots show the number of parasites in 100 cells for each well analyzed. The bars show the mean and SEM. Student's *t* test was used to compare groups. (B) Representative images of iPS-CM transduced with scramble shRNA (top) and shRNA targeting *PPP3CA* after 24 hours of infection with *T. cruzi* expressing GFP (green). Nuclei were labeled with DAPI (gray), and actin was labeled with phalloidin (red).

Chagas disease in Amazonia is mostly enzootic and not endemic, with only sporadic cases occurring in some geographic clusters. Noticeably, the geographic distribution of the allele found under natural selection coincides with the areas of low *T. cruzi* infection in South America (Fig. 3 and fig. S7). In addition, we found a positive correlation between the vector species diversity (Tiatomine) and the frequency of the allele derived (A) for the rs2659540 polymorphism (fig. S8). This result reinforces our hypothesis of natural selection leading to a protective phenotype in Native Americans in this ecosystem, as it suggests a higher potential for infection in the region where the variant is in high frequency.

Brazil alone has approximately 2 million people infected with *T. cruzi* (49). Urban southeastern admixed Brazilians exhibiting African and Native American ancestries were correlated with higher levels of *T. cruzi* infection. However, these two ancestry components were also associated with poor socioeconomic status, making it difficult to dissociate these two factors (50). Nevertheless, the Native American ancestry component of that admixed Brazilians sample has a median contribution of only 5.4% (7.1% infected and 4.8% noninfected); this low ancestry proportion could be another possible confounding factor related to the association between Native American ancestry and high prevalence of Chagas disease. Admixture mapping studies in Colombian admixed populations found a protective association with Chagas disease within the major histocompatibility complex region (51); however, no association was observed with the *PPP3CA* variant. This can be explained by the differences in the ancestry composition of the region that predominantly exhibited an Andean ancestry (52), and wherein the allele found under selection exhibits a lower frequency (0.277). Furthermore, selection did not necessarily occur in the postcontact period; if it did occur, it may not have been strong or widely distributed enough to be detected in admixture mapping analyses. In Southern Mexican populations, several putative genes related to immune and inflammatory responses were identified under natural selection, including *PPP3CA* (53). The forests in this region are abundant with parasites such as *T. cruzi*

and *Leishmania mexicana*, which are endemic. Nevertheless, Southern Native Mexicans are chronically affected by Chagas disease. Individuals affected by this disease show milder progression of the main Chagas-related cardiomyopathies when compared to subjects from other regions of South America. This suggests that there could be alleles under natural selection that could likely be involved in improving disease progression.

Our results provide insights into the population's adaptation to the Amazonian Rainforest. Combining temporal epidemiological data, genomic analyses of selection, the geographic distribution of the putatively selected allele, and functional analysis of the candidate gene, we showed that a variant of the *PPP3CA* gene likely had a protective effect on the infection outcome of Chagas Disease in Amazonian populations in the past, probably due to the reduction in the infection rate of carriers. Moreover, the identification of a role for *PPP3CA* in *T. cruzi* infection contributes to the dissection of the molecular mechanisms of pathogen infection and, thus, potentially to the development of therapies for the disease.

MATERIALS AND METHODS

Dataset assembly

The dataset consists of combined data from 118 non-admixed (Native American ancestry > 0.99) native Amazonians (table S1 and fig. S9), 35 non-admixed Mesoamericans (Native American ancestry > 0.97), and 231 East Asians from the Human Genome Diversity Project (HGDP; dataset 11, <http://cephb.fr/hgdp/>). Samples were genotyped with the high-density SNP array Axiom Human Origins (~700K SNPs, Affymetrix/Thermo Fisher Scientific). Native American ancestry proportions were estimated using ADMIXTURE (54).

Data quality control and phasing

First, we used the liftOver software (<https://genome.ucsc.edu/cgi-bin/hgLiftOver>) to update the physical positions from GRCh37-

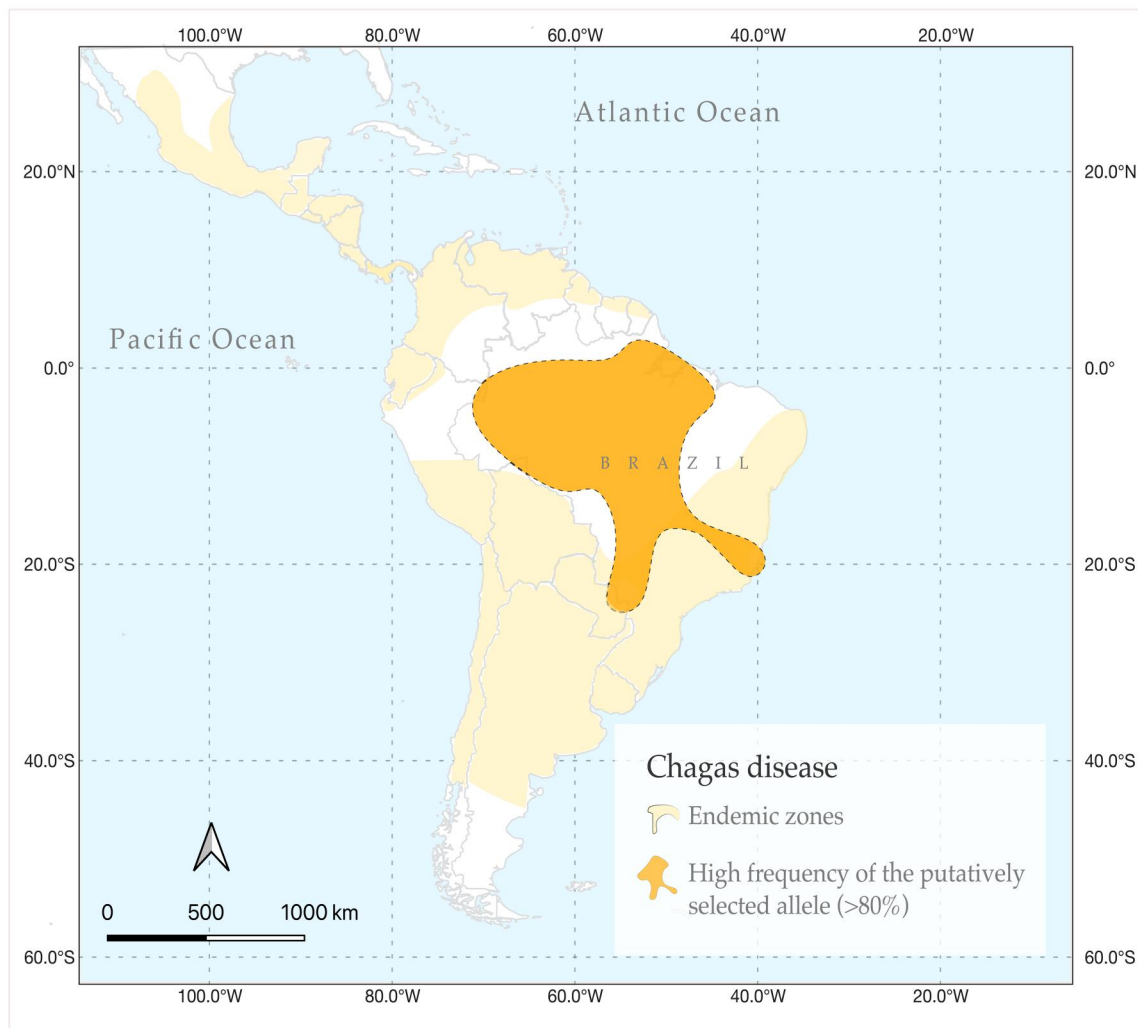


Fig. 3. High-frequency distribution of the putatively selected *PPP3CA* allele. The yellow area on the map represents the endemic region of Chagas disease. The orange area represents the distribution of the putatively selected allele (rs2659540 G>A) in the studied populations.

hg19 to the current genome assembly, GRCh38-hg38. Individuals with more than 10% of missing data and those SNPs with minor allele frequency (MAF) lower than 5% or with more than 1% of missing data were removed. We further computationally phased the data using SHAPEIT2 (55) and the recombination map files from the 1000 Genomes Project (56) to phase the haplotypes. No reference panels were used because of the peculiarities of evolutionary history and the lack of representation of Native American populations in these panels. We used the ancestral and derived allele information annotated in the 1000 Genomes Project from EPO pipeline (56), according to Ensembl FTP site (http://ftp.ensembl.org/pub/release-71/fasta/ancestral_alleles/homo_sapiens_ancestor_GRCh37_e71.tar.bz2), and removed SNPs without such information so that our final phased and polarized datasets contain 517,984 SNPs.

Genome annotation

We used ANNOVAR (57) and in-house scripts for the genome annotation. We annotated gene symbols to each SNP from both

datasets using the RefGene database from ANNOVAR itself, taking 1 Mb as a maximum distance threshold to generate the gene annotation. The SNP IDs were mapped to the publicly available reference from the Axiom Human Origins SNP Array (<https://thermofisher.com/br/en/home/life-science/microarray-analysis/microarray-data-analysis/genechip-array-annotation-files.html>).

Selection scans

To identify the signature of positive selection, we applied methods relying on extended haplotype homozygosity (XP-EHH) and population differentiation (PBS) as described below. We used the phased and polarized dataset to apply Cross Population Extended Haplotype Homozygosity (XP-EHH) statistics, using the rehh R package (22, 58). *P* value normalization was performed using a negative log₁₀ transformation. We structured the XP-EHH analysis using the Native Amazonians as the focal population and the Mesoamericans or East Asians in the comparative analysis.

We also applied the PBS as published by Yi *et al.* (59). Before calculating the PBS values, we removed all monomorphic sites in

at least two of the three analyzed populations, as well as the SNPs with MAF lower than 5% when considering the three populations altogether. We structured our analysis by placing the Native Amazonians as the focal population, Mesoamericans as the sister population, and East Asians as the outgroup. We then applied a rolling-mean approach (window size = 20, steps = 5) to reduce the noise and avoid spurious outliers. For each window, only the SNP with the highest PBS value and its related annotation are reported.

In addition, assuming that selective sweeps leave signatures in adjacent genomic regions, we took a gene approach where we summarized the results by taking the mean of all the SNP PBS values of each gene. We considered as significant those SNPs or genes located in the extreme 99.9th percentile of the distribution (empirical P value from right tail ≤ 0.001). Candidate genes for positive selection were accessed by overlapping XP-EHH greater than 2 (Amazonians \times East Asians and Amazonians \times Mesoamericans) and PBS analysis upper percentile of distribution (99.5th percentile).

Demographic model and simulation

The demographic model (fig. S3A) was built assuming a standstill in Beringia at 26,000 yr B.P., the settlement of America at 15,000 yr B.P., and divergence between Central and South American populations at 13,000 yr B.P. The effective population size and its changes over time were based on the Castro e Silva *et al.* (60) dataset inferred through ASCEND (61) and IBDNe (62) softwares. We assume a mutation rate of 1×10^{-8} and a generation time of 25 years. Demographic simulations for single SNPs were performed using the ms software (63). We used 10,000 simulations according to this scenario to generate a null distribution of the PBS values to which observed PBS values were compared. This procedure allowed us to evaluate the significance of the differences and get the outlier PBS values.

Selection time and intensity

First, to deal with the ascertainment bias of the array data, we imputed [IMPUTE4 (64)] SNPs from chromosome 4 using the HGDP Whole Genome Sequence data as the reference panel (65). Next, 500 kb flanking SNPs adjacent to each side of the candidate SNP (rs2659540) were selected, totaling a 1-Mb genomic region. On the basis of the SNPs observed in this region, DAF (derived allele frequency) and iHS (integrated haplotype score) were inferred (58).

To assess when and the intensity of the selective event in the candidate SNP, we used the msms software (66), with the demographic model described above, assuming that the allele already segregated in populations with a frequency of 0.25 (basal frequency observed in East Asian) and assuming uniform prior distribution for time periods (1000 to 12,500 years) and selection coefficient (0 to 0.2) to simulate 10,000 sequences of 1 Mb each. From the simulated sequences, we selected only the markers in positions also observed in the real data. With this subset of SNPs, the summary statistics DAF and iHS were inferred.

Using the ABC approach, implemented in the abc R package [v.2.2.1 (67)], the parameters that produced the simulated data are accepted or rejected according to the Euclidean distance (ϵ) between observed and simulated summary statistics. As a threshold for the rejection algorithm, for each simulated model, we retained 1% of the top simulations with Euclidean distance between observed and simulated summary statistics closer to zero. The posterior distribution was estimated on the basis of these retained simulations.

Overrepresentation and gene set enrichment analyses

We performed both overrepresentation analysis (ORA) and gene set enrichment analysis (GSEA) on our selection scans' results using the GWAS Catalog (<https://ebi.ac.uk/gwas/>), KEGG Pathway (<https://genome.jp/kegg/pathway.html>), and GO (<http://geneontology.org/docs/go-enrichment-analysis/>) databases. We used WebGestalt (<http://webgestalt.org/>) to apply GSEA, and FUMA GWAS (<https://fuma.ctglab.nl/>), Enrichr (<https://maayanlab.cloud/Enrichr/>), and GO for ORA. The GWAS Catalog database was analyzed using both FUMA GWAS and Enrichr, because FUMA GWAS requires a custom gene background and Enrichr does not. We also used Enrichr alongside GOATOOLS to analyze ORA in the GO database. Last, we used WebGestalt to address GSEA in KEGG. For ORA, we selected genes mapped to SNPs with scan values above the 99.99th, 99.95th, and 99th percentiles, while we used all genes with mean scores for GSEA. Threshold values were set at the minimum necessary to return robust results in the enrichment analysis.

To verify the results found, we used the R package GOfuncR (68), which uses random sets to compute the family-wise error rate (FWER; probability of having at least one false positive when multiple comparisons are being tested), performing a hypergeometric test, taking the gene length and spatial clustering of genes (2-Mb physical distance) in account. We then used a threshold FWER of <0.1 and refined the analyses, removing significant genes and reanalyzing the data to verify that the associated category remains significant.

PPP3CA knockdown hiPSC-derived cardiomyocytes

hiPSCs were differentiated into cardiomyocytes (hiPSC-CM) according to Sharma and collaborators (69). On day 21 of differentiation, hiPSC-CM cells were replated in a 12-well plate (2×10^6 cells per well) for protein analysis or in a 96-well plate (9×10^4 cells per well) for image analysis. On day 28, hiPSC-CM cells were transduced with shRNA lentivirus (MISSION shRNA Lentiviral Transduction Particles, Sigma-Aldrich, #SHCLNV-NM_000944, clones RCN0000352645, TRCN0000342619, TRCN0000352706, TRCN0000002750, and TRCN0000002751) corresponding to five different regions of the protein at a multiplicity of infection (MOI) of 200 for each clone. Scramble shRNA was used as a negative control and was acquired from Addgene (plasmid #1864) gifted by D. Sabatini (70) and transduced at the same MOI. Knockdown was evaluated by the reduction percent measured by Western blot. Then, a radioimmunoprecipitation assay buffer was used to extract the proteins, which were then loaded onto a 4 to 20% gradient bis-tris gel (Novex—Thermo Fisher Scientific). Proteins were transferred to a polyvinylidene difluoride membrane, blocked with 5% fat-free milk in 0.5% phosphate buffered saline tween® (PBST), and probed using PPP3CA (Abcam, #ab3673) or glyceraldehyde-3-phosphate dehydrogenase (GAPDH) (Santa Cruz Biotechnology, sc-32233) antibodies.

Infection of hiPSC-CM by *T. cruzi*

T. cruzi [Y strain—green fluorescent protein (GFP)—tag (71)] trypanomastigote form from LCMK2 supernatant was inoculated in human induced pluripotent stem cell-derived cardiomyocytes (iPS-CM) 48 hours after the shRNA transfection at MOI of 5. For infection analysis [24 hours post infection (hpi)], cells were fixed with 4% paraformaldehyde after phosphate-buffered saline washes. For image

analysis, cells were stained with 4',6-diamidino-2-phenylindole (DAPI) for nuclei labeling and Alexa Fluor 555-phalloidin (Thermo Fisher Scientific, #A34055) for cytoskeleton labeling. Images were captured at a magnification of $\times 20$ using Molecular Devices IXM-C high-content screening.

We acquired 12 images per well, five wells per differentiation, and two independent differentiations per infection. Nuclei and parasites were counted using MATLAB and are the sum of 12 images of each well. After 24 hours of infection, we counted the number of parasites inside the cells in each well. We analyzed 10 wells with negative control shRNA (scrambled) and 10 wells with shRNA targeting *PPP3CA*, and each dot in Fig. 2 is the measure of one well. We performed a *t* test to compare the number of parasites that infected cells in each group.

Correlation analysis

To investigate the correlation of the geographic distribution of the putative-selected allele (rs2659540 G>A) and Chagas disease, we performed two analyses. In the first, from the geographic coordinates of each population analyzed on the present study, we used data from geographic distribution models of the number of Chagas disease vectors (Triatomine species), described by (13) and (72) and correlated with the frequency of the putatively selected rs2659540 G>A in different geographic regions. In the second analysis, we correlated data on the incidence rate (cases per 100,000 population) of Chagas disease in different regions of Brazil (Sistema de Informação de Agravos de Notificação SINAN, Brazilian Ministry of Health) and Mexico (73), between the years 2003 and 2013, and the frequency of the candidate allele rs2659540 G>A. Correlation analysis was performed in R language with the stats package.

Supplementary Materials

This PDF file includes:

Figs. S1 to S9

Legends for tables S1 to S5

References

Other Supplementary Material for this

manuscript includes the following:

Tables S1 to S5

[View/request a protocol for this paper from Bio-protocol.](#)

REFERENCES AND NOTES

1. B. Llamas, L. Fehren-Schmitz, G. Valverde, J. Soubrier, S. Mallick, N. Rohland, S. Nordenfellt, C. Valdiosera, S. M. Richards, A. Rohrlach, M. I. B. Romero, I. F. Espinoza, E. T. Cagigao, L. W. Jiménez, K. Makowski, I. S. L. Reyna, J. M. Lory, J. A. B. Torrez, M. A. Rivera, R. L. Burger, M. C. Ceruti, J. Reinhard, R. S. Wells, G. Politis, C. M. Santoro, V. G. Standen, C. Smith, D. Reich, S. Y. W. Ho, A. Cooper, W. Haak, Ancient mitochondrial DNA provides high-resolution time scale of the peopling of the Americas. *Sci. Adv.* **2**, e1501385 (2016).
2. V. Acuña-Alonzo, T. Flores-Dorantes, J. K. Kruit, T. Villarreal-Molina, O. Arellano-Campos, T. Hünemeier, A. Moreno-Estrada, M. G. Ortiz-López, H. Villamil-Ramírez, P. León-Mimila, M. Villalobos-Companan, L. Jacobo-Albavera, S. Ramírez-Jiménez, M. Sikora, L.-H. Zhang, T. D. Pape, M. d. A. Granados-Silvestre, I. Montufar-Robles, A. M. Tito-Alvarez, C. Zurita-Salinas, J. Bustos-Arriaga, L. Cedillo-Barrón, C. Gómez-Trejo, R. Barquera-Lozano, J. P. Vieira-Filho, J. Granados, S. Romero-Hidalgo, A. Huertas-Vázquez, A. González-Martín, A. Gorostiza, S. L. Bonatto, M. Rodríguez-Cruz, L. Wang, T. Tusié-Luna, C. A. Aguilar-Salinas, R. Lisker, R. S. Moises, M. Menjivar, F. M. Salzano, W. C. Knowler, M. C. Bortolini, M. R. Hayden, L. J. Baier, S. Canizales-Quinteros, A functional *ABCA1* gene variant is associated with low HDL-cholesterol levels and shows evidence of positive selection in Native Americans. *Hum. Mol. Genet.* **19**, 2877–2885 (2010).
3. T. Hünemeier, C. E. G. Amorim, S. Azevedo, V. Contini, V. Acuña-Alonzo, F. Rothhammer, J.-M. Dugoujon, S. Mazières, R. Barrantes, M. T. Villarreal-Molina, V. R. Paixão-Côrtés, F. M. Salzano, S. Canizales-Quinteros, A. Ruiz-Linares, M. C. Bortolini, Evolutionary responses to a constructed niche: Ancient Mesoamericans as a model of gene-culture co-evolution. *PLOS ONE* **7**, e38862 (2012).
4. C. E. G. Amorim, K. Nunes, D. Meyer, D. Comas, M. C. Bortolini, F. M. Salzano, T. Hünemeier, Genetic signature of natural selection in first Americans. *Proc. Natl. Acad. Sci. U.S.A.* **114**, 2195–2199 (2017).
5. J. Lindo, R. Haas, C. Hofman, M. Apatá, M. Moraga, R. A. Verdugo, J. T. Watson, C. Viviano Llave, D. Witonsky, C. Beall, C. Warinner, J. Novembre, M. Aldenderfer, A. Di Rienzo, The genetic prehistory of the Andean highlands 7000 years BP though European contact. *Sci. Adv.* **4**, eaau4921 (2018).
6. T. B. Hart, J. A. Hart, The ecological basis of hunter-gatherer subsistence in African rain forests: The Mbuti of Eastern Zaire, in *Case Studies in Human Ecology*, D. G. Bates, S. H. Lees, Eds. (Springer, 1996), pp. 55–83.
7. R. C. Bailey, G. Head, M. Jenike, B. Owen, R. Rechtman, E. Zechenter, Hunting and gathering in tropical rain forest: Is it possible? *Am. Anthropol.* **91**, 59–82 (1989).
8. J. Ratnam, W. J. Bond, R. J. Fensham, W. A. Hoffmann, S. Archibald, C. E. R. Lehmann, M. T. Anderson, S. I. Higgins, M. Sankaran, When is a “forest” a savanna, and why does it matter? *Glob. Ecol. Biogeogr.* **20**, 653–660 (2011).
9. V. Guernier, M. E. Hochberg, J.-F. Guégan, Ecology drives the worldwide distribution of human diseases. *PLOS Biol.* **2**, e141 (2004).
10. F. M. Salzano, *The Amerindian Microcosm: Anthropology, Comparative History, Ecology, Genetics and Evolution* (Cambridge Scholars Publishing, 2019).
11. P. L. Taail, The status of infectious disease in the Amazon region. *Emerg. Infect. Dis.* **15**, 625 (2009).
12. U. E. C. Confalonieri, C. Margonari, A. F. Quintão, Environmental change and the dynamics of parasitic diseases in the Amazon. *Acta Trop.* **129**, 33–41 (2014).
13. F. E. Eberhard, S. Cunze, J. Kochmann, S. Klimpel, Modelling the climatic suitability of Chagas disease vectors on a global scale. *eLife* **9**, e2072 (2020).
14. R. Walker, L. Sattenspiel, K. Hill, Mortality from contact-related epidemics among indigenous populations in Greater Amazonia. *Sci. Rep.* **5**, 14032 (2015).
15. M. J. Allison, D. Mendoza, A. Pezzia, Documentation of a case of tuberculosis in Pre-Columbian America. *Am. Rev. Respir. Dis.* **107**, 985–991 (1973).
16. J. E. Buikstra, S. Williams, Tuberculosis in the Americas: Current perspectives, in *Human Paleopathology, Current Syntheses and Future Options*, D. Ortner, A. Aufderheide, Eds. (Smithsonian Institution Press, Washington DC, ed. 1, 1991), pp. 161–172.
17. F. Guhl, C. Jaramillo, R. Yockteng, G. A. Vallejo, F. Cárdenas-Arroyo, Trypanosoma cruzi DNA in human mummies. *Lancet* **349**, 1370 (1997).
18. A. C. Aufderheide, W. Salo, M. Madden, J. Streitz, J. Buikstra, F. Guhl, B. Arriaza, C. Renier, L. E. Wittmers Jr., G. Fornaciari, M. Allison, A 9,000-year record of Chagas' disease. *Proc. Natl. Acad. Sci. U.S.A.* **101**, 2034–2039 (2004).
19. V. S. Lima, A. M. Iniguez, K. Otsuki, L. Fernando Ferreira, A. Araújo, A. C. P. Vicente, A. M. Jansen, Chagas disease in ancient hunter-gatherer population, Brazil. *Emerg. Infect. Dis.* **14**, 1001–1002 (2008).
20. C. E. G. Amorim, J. T. Daub, F. M. Salzano, M. Foll, L. Excoffier, Detection of convergent genome-wide signals of adaptation to tropical forests in humans. *PLOS ONE* **10**, e0121557 (2015).
21. V. Borda, I. Alvim, M. Mendes, C. Silva-Carvalho, G. B. Soares-Souza, T. P. Leal, V. Furlan, M. O. Scliar, R. Zamudio, C. Zolini, G. S. Araújo, M. R. Luizon, C. Padilla, O. Cáceres, K. Levano, C. Sánchez, O. Trujillo, P. O. Flores-Villanueva, M. Dean, S. Fuselli, M. Machado, P. E. Romero, F. Tassi, M. Yeager, T. D. O'Connor, R. H. Gilman, E. Tarazona-Santos, H. Guio, The genetic structure and adaptation of Andean highlanders and Amazonians are influenced by the interplay between geography and culture. *Proc. Natl. Acad. Sci. U.S.A.* **117**, 32557–32565 (2020).
22. M. Gautier, R. Vitalis, rehh: An R package to detect footprints of selection in genome-wide SNP data from haplotype structure. *Bioinformatics* **28**, 1176–1177 (2012).
23. K. Watanabe, E. Taskesen, A. van Bochoven, D. Posthuma, Functional mapping and annotation of genetic associations with FUMA. *Nat. Commun.* **8**, 1826 (2017).
24. H. Mi, A. Muruganujan, D. Ebert, X. Huang, P. D. Thomas, PANTHER version 14: More genomes, a new PANTHER GO-slim and improvements in enrichment analysis tools. *Nucleic Acids Res.* **47**, D419–D426 (2019).
25. H. Ogata, S. Goto, K. Sato, W. Fujibuchi, H. Bono, M. Kanehisa, KEGG: Kyoto Encyclopedia of Genes and Genomes. *Nucleic Acids Res.* **27**, 29–34 (1999).
26. J. Griss, G. Viteri, K. Sidiropoulos, V. Nguyen, A. Fabregat, H. Hermjakob, ReactomeGSA-efficient multi-omics comparative pathway analysis. *Mol. Cell. Proteomics* **19**, 2115–2125 (2020).
27. B. Zhang, S. Kirov, J. Snoddy, WebGestalt: An integrated system for exploring gene sets in various biological contexts. *Nucleic Acids Res.* **33**, W741–W748 (2005).

28. R. B. Kennedy, I. G. Ovsyannikova, V. S. Pankratz, I. H. Haralambieva, R. A. Vierkant, G. A. Poland, Genome-wide analysis of polymorphisms associated with cytokine responses in smallpox vaccine recipients. *Hum. Genet.* **131**, 1403–1421 (2012).
29. A. V. Jones, M. Tilley, A. Gutteridge, C. Hyde, M. Nagle, D. Ziemek, D. Gorman, E. B. Fauman, X. Chen, M. R. Miller, GWAS of self-reported mosquito bite size, itch intensity and attractiveness to mosquitoes implicates immune-related predisposition loci. *Hum. Mol. Genet.* **26**, 1391–1406 (2017).
30. D. N. Harris, W. Song, A. C. Shetty, K. S. Levano, O. Cáceres, C. Padilla, V. Borda, D. Tarazona, O. Trujillo, C. Sanchez, M. D. Kessler, M. Galarza, S. Capristano, H. Montejo, P. O. Flores-Villanueva, E. Tarazona-Santos, T. D. O'Connor, H. Guio, Evolutionary genomic dynamics of Peruvians before, during, and after the Inca Empire. *Proc. Natl. Acad. Sci. U.S.A.* **115**, E6526–E6535 (2018).
31. A. E. P. Lourenço, R. V. Santos, J. D. Y. Orellana, C. E. A. Coimbra, Nutrition transition in Amazonia: Obesity and socioeconomic change in the Suruí Indians from Brazil. *Am. J. Hum. Biol.* **20**, 564–571 (2008).
32. S. G. A. Gimeno, D. Rodrigues, E. N. Canó, E. E. S. Lima, M. Schaper, H. Pagliaro, M. M. Lafer, R. G. Baruzzi, Cardiovascular risk factors among Brazilian Karib indigenous peoples: Upper Xingu, Central Brazil, 2000–3. *J. Epidemiol. Community Health* **63**, 299–304 (2009).
33. L. P. Soares, A. L. D. Fabbro, A. S. Silva, D. S. Sartorelli, L. F. Franco, P. C. Kuhn, R. S. Moises, J. P. B. Vieira-Filho, L. J. Franco, Prevalence of metabolic syndrome in the Brazilian Xavante indigenous population. *Diabetol. Metab. Syndr.* **7**, 105 (2015).
34. C. M. Bergey, M. Lopez, G. F. Harrison, E. Patin, J. A. Cohen, L. Quintana-Murci, L. B. Barreiro, G. H. Perry, Polygenic adaptation and convergent evolution on growth and cardiac genetic pathways in African and Asian rainforest hunter-gatherers. *Proc. Natl. Acad. Sci. U.S.A.* **115**, E11256–E11263 (2018).
35. R. Redolat, A. Perez-Martinez, M. Carrasco, P. Mesa, Individual differences in novelty-seeking and behavioral responses to nicotine: A review of animal studies. *Curr. Drug Abuse Rev.* **2**, 230–242 (2009).
36. T. Wingo, T. Nesil, J.-S. Choi, M. D. Li, Novelty seeking and drug addiction in humans and animals: From behavior to molecules. *J. Neuroimmune Pharmacol.* **11**, 456–470 (2016).
37. L. Tovo-Rodrigues, S. M. Callegari-Jacques, M. L. Petzl-Erler, L. Tsuneto, F. M. Salzano, M. H. Hutz, Dopamine receptor D4 allele distribution in Amerindians: A reflection of past behavior differences? *Am. J. Phys. Anthropol.* **143**, 458–464 (2010).
38. A. de Rubira, L. Georges, L. Fehren-Schmitz, Ancient DNA reveals that the variability of the DRD4-521 C/T SNP associated with novelty seeking behavior is influenced by selection in Western South American populations. *Adapt. Hum. Behav. Physiol.* **2**, 77–91 (2016).
39. S. Feske, H. Okamura, P. G. Hogan, A. Rao, Ca^{2+} /calcineurin signalling in cells of the immune system. *Biochem. Biophys. Res. Commun.* **311**, 1117–1132 (2003).
40. P. R. Orrego, H. Olivares, E. M. Cordero, A. Bressan, M. Cortez, H. Sagua, I. Neira, J. González, J. F. da Silveira, N. Yoshida, J. E. Araya, A cytoplasmic new catalytic subunit of calcineurin in *Trypanosoma cruzi* and its molecular and functional characterization. *PLOS Negl. Trop. Dis.* **8**, e2676 (2014).
41. T. Mizuguchi, M. Nakashima, M. Kato, N. Okamoto, H. Kurahashi, N. Ekhilevitch, M. Shiina, G. Nishimura, T. Shibata, M. Matsuo, Loss-of-function and gain-of-function mutations in PPP3CA cause two distinct disorders. *Hum. Mol. Genet.* **27**, 1421–1433 (2018).
42. M. C. P. Nunes, A. Beaton, H. Acquatella, C. Bern, A. F. Bolger, L. E. Echeverría, W. O. Dutra, J. Gascon, C. A. Morillo, J. A. Oliveira-Filho, A. L. P. Ribeiro, J. A. Marin-Neto; American Heart Association Rheumatic Fever; Endocarditis and Kawasaki Disease Committee of the Council on Cardiovascular Disease in the Young; Council on Cardiovascular and Stroke Nursing; and Stroke Council, Chagas cardiomyopathy: An update of current clinical knowledge and management: A scientific statement from the American Heart Association. *Circulation* **138**, e169–e209 (2018).
43. V. D. Aiello, F. P. F. de Campos, Chronic Chagas cardiomyopathy. *Autops. Case Rep.* **5**, 7–9 (2015).
44. J. S. Rees, S. Castellano, A. M. Andrés, The genomics of human local adaptation. *Trends Genet.* **36**, 415–428 (2020).
45. C. de Filippo, F. M. Key, S. Ghirotto, A. Benazzo, J. R. Meneu, A. Weihmann; NISC Comparative Sequence Program, G. Parra, E. D. Green, A. M. Andrés, Recent selection changes in human genes under long-term balancing selection. *Mol. Biol. Evol.* **33**, 1435–1447 (2016).
46. K. C. F. Lidani, F. A. Andrade, L. Bavia, F. S. Damasceno, M. H. Beltrame, I. J. Messias-Reason, T. L. Sandri, Chagas disease: From discovery to a worldwide health problem. *Front. Public Health* **7**, 166 (2019).
47. J. Pèneau, A. Nguyen, A. Flores-Ferrer, D. Blanchet, S. Gourbière, Amazonian triatomine biodiversity and the transmission of chagas disease in french Guiana: In Medio Stat Sanitas. *PLOS Negl. Trop. Dis.* **10**, e0004427 (2016).
48. R. V. Santos, C. ampt;Epsilon; A. Coimbra Jr, *Saúde e Povos Indígenas* (Editora FIOCRUZ, 1994).
49. A. R. de Arias, C. Monroy, F. Guhl, S. Sosa-Estani, W. S. Santos, F. Abad-Franch, Chagas disease control-surveillance in the Americas: The multinational initiatives and the practical impossibility of interrupting vector-borne *Trypanosoma cruzi* transmission. *Mem. Inst. Oswaldo Cruz* **117**, e210130 (2022).
50. M. F. Lima-Costa, J. Macinko, J. V. d. M. Mambrini, S. V. Peixoto, A. C. Pereira, E. Tarazona-Santos, A. L. P. Ribeiro, Genomic African and Native American ancestry and chagas disease: The Bambui (Brazil) epigen cohort study of aging. *PLOS Negl. Trop. Dis.* **10**, e0004724 (2016).
51. D. Casares-Marfil, B. Guillen-Guio, J. M. Lorenzo-Salazar, H. Rodríguez-Pérez, M. Kerick, M. A. Jaimes-Campos, M. L. Díaz, E. Estupiñán, L. E. Echeverría, C. I. González, J. Martín, C. Flores, M. Acosta-Herrera, Admixture mapping analysis reveals differential genetic ancestry associated with Chagas disease susceptibility in the Colombian population. *Hum. Mol. Genet.* **30**, 2503–2512 (2021).
52. H. Ossa, J. Aquino, R. Pereira, A. Ibarra, R. H. Ossa, L. A. Pérez, J. D. Granda, M. C. Lattig, H. Groot, E. F. de Carvalho, L. Gusmão, Outlining the ancestry landscape of Colombian admixed populations. *PLOS ONE* **11**, e0164414 (2016).
53. C. Ojeda-Granados, P. Abondio, A. Setti, S. Sarno, G. A. Gnecci-Ruscone, E. González-Orozco, S. De Fanti, A. Jiménez-Kaufmann, H. Rangel-Villalobos, A. Moreno-Estrada, M. Sazzini, Dietary, cultural, and pathogens-related selective pressures shaped differential adaptive evolution among native Mexican populations. *Mol. Biol. Evol.* **39**, msab290 (2022).
54. D. H. Alexander, J. Novembre, K. Lange, Fast model-based estimation of ancestry in unrelated individuals. *Genome Res.* **19**, 1655–1664 (2009).
55. O. Delaneau, J.-F. Zagury, J. Marchini, Improved whole-chromosome phasing for disease and population genetic studies. *Nat. Methods* **10**, 5–6 (2013).
56. 1000 Genomes Project Consortium, A. Auton, L. D. Brooks, R. M. Durbin, E. P. Garrison, H. M. Kang, J. O. Korbel, J. L. Marchini, S. McCarthy, G. A. McVean, G. R. Abecasis, A global reference for human genetic variation. *Nature* **526**, 68–74 (2015).
57. K. Wang, M. Li, H. Hakonarson, ANNOVAR: Functional annotation of genetic variants from high-throughput sequencing data. *Nucleic Acids Res.* **38**, e164 (2010).
58. M. Gautier, A. Klassmann, R. Vitalis, rehh 2.0: A reimplementation of the R package rehh to detect positive selection from haplotype structure. *Mol. Ecol. Resour.* **17**, 78–90 (2017).
59. X. Yi, Y. Liang, E. Huerta-Sanchez, X. Jin, Z. X. P. Cuo, J. E. Pool, X. Xu, H. Jiang, N. Vinckenbosch, T. S. Korneliussen, H. Zheng, T. Liu, W. He, K. Li, R. Luo, X. Nie, H. Wu, M. Zhao, H. Cao, J. Zou, Y. Shan, S. Li, Q. Yang, Asan, P. Ni, G. Tian, J. Xu, X. Liu, T. Jiang, R. Wu, G. Zhou, M. Tang, J. Qin, T. Wang, S. Feng, G. Li, Huasang, J. Luosang, W. Wang, F. Chen, Y. Wang, X. Zheng, Z. Li, Z. Bianba, G. Yang, X. Wang, S. Tang, G. Gao, Y. Chen, Z. Luo, L. Gusang, Z. Cao, Q. Zhang, W. Ouyang, X. Ren, H. Liang, H. Zheng, Y. Huang, J. Li, L. Bolund, K. Kristiansen, Y. Li, Y. Zhang, X. Zhang, R. Li, S. Li, H. Yang, R. Nielsen, J. Wang, J. Wang, Sequencing of 50 human exomes reveals adaptation to high altitude. *Science* **329**, 75–78 (2010).
60. M. A. C. e. Silva, T. Ferraz, C. M. Couto-Silva, R. B. Lemes, K. Nunes, D. Comas, T. Hünemeier, Population histories and genomic diversity of south American natives. *Mol. Biol. Evol.* **39**, msab339 (2022).
61. R. Tournebize, G. Chu, P. Moorjani, Reconstructing the history of founder events using genome-wide patterns of allele sharing across individuals. *PLOS Genet.* **18**, e1010243 (2022).
62. S. R. Browning, B. L. Browning, Accurate non-parametric estimation of recent effective population size from segments of identity by descent. *Am. J. Hum. Genet.* **97**, 404–418 (2015).
63. R. R. Hudson, Generating samples under a Wright-Fisher neutral model of genetic variation. *Bioinformatics* **18**, 337–338 (2002).
64. C. Bycroft, C. Freeman, D. Petkova, G. Band, L. T. Elliott, K. Sharp, A. Motyer, D. Vukcevic, O. Delaneau, J. O'Connell, A. Cortes, S. Welsh, A. Young, M. Effingham, G. McVean, S. Leslie, N. Allen, P. Donnelly, J. Marchini, The UK Biobank resource with deep phenotyping and genomic data. *Nature* **562**, 203–209 (2018).
65. A. Bergstrom, S. A. McCarthy, R. Hui, M. A. Almarri, Q. Ayub, P. Danecek, Y. Chen, S. Felkel, P. Hallast, J. Kamm, H. Blanche, J. F. Deleuze, H. Cann, S. Mallick, D. Reich, M. S. Sandhu, P. Skoglund, A. Scally, Y. Xue, R. Durbin, C. Tyler-Smith, Insights into human genetic variation and population history from 929 diverse genomes. *Science* **367**, eaay5012 (2020).
66. G. Ewing, J. Hermisson, MSMS: A coalescent simulation program including recombination, demographic structure and selection at a single locus. *Bioinformatics* **26**, 2064–2065 (2010).
67. K. Csilléry, O. François, M. G. B. Blum, abc: An R package for approximate Bayesian computation (ABC). *Methods Ecol. Evol.* **3**, 475–479 (2012).
68. S. Grote, GOfuncR: Gene Ontology Enrichment Using FUNC, R package version 1.18.0; <https://bioconductor.org/packages/release/bioc/html/GOfuncR.html>.
69. A. Sharma, C. N. Toepfer, M. Schmid, A. C. Garfinkel, C. E. Seidman, Differentiation and contractile analysis of GFP-sarcomere reporter hiPSC-cardiomyocytes. *Curr. Protoc. Hum. Genet.* **96**, 21.12.1–21.12.12 (2018).

70. D. D. Sarbassov, D. A. Guertin, S. M. Ali, D. M. Sabatini, Phosphorylation and regulation of Akt/PKB by the Rictor-mTOR complex. *Science* **307**, 1098–1101 (2005).
71. M. I. Ramirez, L. M. Yamauchi, L. H. de Freitas Jr, H. Uemura, S. Schenkman, The use of the green fluorescent protein to monitor and improve transfection in *Trypanosoma cruzi*. *Mol. Biochem. Parasitol.* **111**, 235–240 (2000).
72. F. A. Monteiro, C. Weirauch, M. Felix, C. Lazoski, F. Abad-Franch, Evolution, systematics, and biogeography of the triatominae, vectors of Chagas disease. *Adv. Parasitol.* **99**, 265–344 (2018).
73. E. M. Shelly, R. Acuna-Soto, K. C. Ernst, C. R. Sterling, H. E. Brown, A critical assessment of officially reported Chagas disease surveillance data in Mexico. *Public Health Rep.* **131**, 59–66 (2016).
74. P. Skoglund, S. Mallick, M. C. Bortolini, N. Chennagiri, T. Hünemeier, M. L. Petzl-Erler, F. M. Salzano, N. Patterson, D. Reich, Genetic evidence for two founding populations of the Americas. *Nature* **525**, 104–108 (2015).
75. M. Araújo Castro E. Silva, T. Ferraz, M. C. Bortolini, D. Comas, T. Hünemeier, Deep genetic affinity between coastal Pacific and Amazonian natives evidenced by Australasian ancestry. *Proc. Natl. Acad. Sci. U.S.A.* **118**, e2025739118 (2021).
76. M. A. Castro E. Silva, K. Nunes, R. B. Lemes, A. Mas-Sandoval, C. E. G. Amorim, J. E. Krieger, J. G. Mill, F. M. Salzano, M. C. Bortolini, A. D. C. Pereira, D. Comas, T. Hünemeier, Genomic insight into the origins and dispersal of the Brazilian coastal natives. *Proc. Natl. Acad. Sci. U.S.A.* **117**, 2372–2377 (2020).
77. N. Patterson, P. Moorjani, Y. Luo, S. Mallick, N. Rohland, Y. Zhan, T. Genschoreck, T. Webster, D. Reich, Ancient admixture in human history. *Genetics* **192**, 1065–1093 (2012).
78. X. Deng, E. C. Sabino, E. Cunha-Neto, A. L. Ribeiro, B. Ianni, C. Mady, M. P. Busch, M. Seielstad, Genome wide association study (GWAS) of Chagas cardiomyopathy in *Trypanosoma cruzi* seropositive subjects. *PLOS ONE* **8**, e79629 (2013).
79. A. Xu, W. Wang, X. Jiang, The roles of *MTRR* and *MTHFR* gene polymorphisms in congenital heart diseases: A meta-analysis. *Biosci. Rep.* **38**, BSR20181160 (2018).
80. Y. R. Kim, S.-H. Hong, Associations of *MTRR* and *TSER* polymorphisms related to folate metabolism with susceptibility to metabolic syndrome. *Genes Genomics* **41**, 983–991 (2019).
81. A. P. Sowton, N. Padmanabhan, S. J. Tunster, B. D. McNally, A. Murgia, A. Yusuf, J. L. Griffin, A. J. Murray, E. D. Watson, *Mtrr* hypomorphic mutation alters liver morphology, metabolism and fuel storage in mice. *Mol. Genet. Metab. Rep.* **23**, 100580 (2020).
82. H. Jiao, P. Arner, J. Hoffstedt, D. Brodin, B. Dubern, S. Czernichow, F. van't Hooft, T. Axelsson, O. Pedersen, T. Hansen, T. I. A. Sørensen, J. Hebebrand, J. Kere, K. Dahlman-Wright, A. Hamsten, K. Clement, I. Dahlman, Genome wide association study identifies *KCNMA1* contributing to human obesity. *BMC Med. Genomics* **4**, 51 (2011).
83. S. K. Iyengar, J. R. Sedor, B. I. Freedman, W. H. L. Kao, M. Kretzler, B. J. Keller, H. E. Abboud, S. G. Adler, L. G. Best, D. W. Bowden, A. Burlock, Y.-D. I. Chen, S. A. Cole, M. E. Comeau, J. M. Curtis, J. Divers, C. Drechsler, R. Duggirala, R. C. Elston, X. Guo, H. Huang, M. M. Hoffmann, B. V. Howard, E. Ipp, P. L. Kimmel, M. J. Klag, W. C. Knowler, O. F. Kohn, T. S. Leak, D. J. Leehey, M. Li, A. Malhotra, W. März, V. Nair, R. G. Nelson, S. B. Nicholas, S. J. O'Brien, M. V. Pahl, R. S. Parekh, M. G. Pezzolesi, R. S. Rasooly, C. N. Rotimi, J. I. Rotter, J. R. Schelling, M. F. Seldin, V. O. Shah, A. M. Smiles, M. W. Smith, K. D. Taylor, F. Thameem, D. P. Thornley-Brown, B. J. Truitt, C. Wanner, E. J. Weil, C. A. Winkler, P. G. Zager, R. P. Igo Jr, R. L. Hanson, C. D. Langefeld, Family investigation of nephropathy and diabetes (find), genome-wide association and trans-ethnic meta-analysis for advanced diabetic kidney disease: Family investigation of nephropathy and diabetes (FIND). *PLOS Genet.* **11**, e1005352 (2015).
84. E. Dahlström, N. Sandholm, Progress in defining the genetic basis of diabetic complications. *Curr. Diab. Rep.* **17**, 80 (2017).
85. F. Liu, L. I. U. Fengzhi, H. Shinomiya, T. Kirikae, H. Hirata, Y. Asano, Characterization of murine grancalcin specifically expressed in leukocytes and its possible role in host defense against bacterial infection. *Biosci. Biotechnol. Biochem.* **68**, 894–902 (2004).
86. P. Xu, J. Roes, A. W. Segal, M. Radulovic, The role of grancalcin in adhesion of neutrophils. *Cell. Immunol.* **240**, 116–121 (2006).
87. T. W. Kim, S. Hong, A. H. Talukder, V. Pascual, Y.-J. Liu, Grancalcin (GCA) modulates Toll-like receptor 9 (TLR9) mediated signaling through its direct interaction with TLR9. *Eur. J. Immunol.* **46**, 712–724 (2016).
88. C. Robichon, M. Varret, X. Le Liepvre, F. Lasnier, E. Hajdouch, P. Ferré, I. Dugail, DnaJA4 is a SREBP-regulated chaperone involved in the cholesterol biosynthesis pathway. *Biochim. Biophys. Acta* **1761**, 1107–1113 (2006).
89. R. J. O'Brien, I. Loke, J. E. Davies, I. B. Squire, L. L. Ng, Myotrophin in human heart failure. *J. Am. Coll. Cardiol.* **42**, 719–725 (2003).
90. I. Seim, S. L. Carter, A. C. Herington, L. K. Chopin, Complex organisation and structure of the ghrelin antisense strand gene *GHRLOS*, a candidate non-coding RNA gene. *BMC Mol. Biol.* **9**, 95 (2008).
91. W.-H. Wei, G. Hemani, A. Gyenesei, V. Vitart, P. Navarro, C. Hayward, C. P. Cabrera, J. E. Huffman, S. A. Knott, A. A. Hicks, I. Rudan, P. P. Pramstaller, S. H. Wild, J. F. Wilson, H. Campbell, N. D. Hastie, A. F. Wright, C. S. Haley, Genome-wide analysis of epistasis in body mass index using multiple human populations. *Eur. J. Hum. Genet.* **20**, 857–862 (2012).

Acknowledgments: We thank C. E. G. Amorim and M. C. Bortolini for comments and suggestions, O. Lao for his help in the analysis, and T. Ferraz for graphic assistance. We also thank all the native communities who participated in the study. **Funding:** This work was supported by São Paulo Research Foundation (FAPESP) grants 17/14916-8 (to C.M.C.-S.), 15/26875-9 (T.H.), and 19/11821-1 (to G.V.), NHLBI R01HL133165 (to A.P.), and NIH grants R01GM075091(to K.N.) and SU19AI098461 (to A.P.). **Author contributions:** Conceptualization: T.H. Methodology: C.M.C.-S., K.N., L.V.P., and A.P. Investigation: C.M.C.-S., K.N., G.V., and T.H. Funding acquisition: D.C., A.P., and T.H. Project administration: T.H. Supervision: T.H. Writing—original draft: K.N., M.A.C.e.S., L.V.P., A.P., and T.H. Writing—review and editing: T.H. **Competing interests:** The authors declare that they have no competing interests. **Data and materials availability:** All data needed to evaluate the conclusions in the paper are present in the paper and/or the Supplementary Materials. The in house scripts for gene adaptation can be found at https://zenodo.org/record/7620975#.Y_Don3bMI2x.

Submitted 7 January 2022
Accepted 8 February 2023
Published 8 March 2023
10.1126/sciadv.abo0234